High-Yield Synthesis of Single-Crystalline Antimony Telluride Hexagonal Nanoplates Using a Solvothermal Approach

ARTICLE *in* JOURNAL OF THE AMERICAN CHEMICAL SOCIETY · NOVEMBER 2005

Impact Factor: 12.11 · DOI: 10.1021/ja054861p · Source: PubMed

J|A|C|S
COMMUNICATIONS

Published on Web 09/17/2005

High-Yield Synthesis of Single-Crystalline Antimony Telluride Hexagonal Nanoplates Using a Solvothermal Approach

Wenzhong Wang,* Bed Poudel, Jian Yang, D. Z. Wang, and Z. F. Ren*

Department of Physics, Boston College, Chestnut Hill, Massachusetts 02467

Received July 20, 2005; E-mail: renzh@bc.edu; wangwm@bc.edu

There is a growing interest in nanostructured thermoelectric (TE) materials since both theoretical predictions[1,2] and experimental results[3,4] suggest that large improvements in figure-of-merit (ZT) could be achieved in nanostructured systems. If the ZT is improved to be ~3, then TE coolers and power generators will become competitive with conventional compressor-based refrigerators and power sources.[5] Antimony telluride (Sb_2Te_3) belongs to layered semiconductors with tetradymite structure. This compound and its doped derivatives are considered to be the best candidates for near room-temperature TE applications.[6] For instance, specially constructed Bi_2Te_3/Sb_2Te_3 superlattices were reported to exhibit a ZT of ~2.4 at room temperature.[6] However, so far, there are only a few reports on the synthesis of polycrystalline Sb_2Te_3 nanowires using electrochemical deposition into the channels of the porous anodic alumina membrane.[7]It is therefore essential to develop an alternative approach to prepare a large quantity of nanosized single-crystalline Sb_2Te_3 materials to meet the demand of high-performance TE applications.

Although various chemical methods have so far been developed to prepare nanostructured materials with different platelike shapes, these methods mainly focus on the fabrication of metal nanostructured materials, such as Ag nanoplates,[8,9] Ag nanodisks,[10,11] Au nanodisks,[12] Au nanoplates.[13−15] It was reported that hexagonal platelet-like Bi_2Te_3 and Bi_2Se_3 nanocrystals could be prepared by a high-temperature organic solution approach[16] and a hydrothermal process,[17] respectively. Here, we report a high-yield solution-based synthesis of two-dimensional (2D) hexagonal nanoplates of Sb_2Te_3.

The hexagonal-shaped Sb_2Te_3 2D nanoplates were prepared by the following procedure: 1.1 mmol of hexadecyltrimethylammonium bromide (CTAB) was dissolved into 10 mL of distilled water with the help of continuous magnetic stirring, then 80 mL of ethanol was added. The solution was stirred for 10 min, then 10 mmol of $SbCl_3$ was added and dissolved completely, followed by addition 15 mmol of Te powder and 20 mmol of $NaBH_4$ and stirring for 15 min. The mixtures were transferred into a Parr reactor, sealed, and kept at 200 °C for 24 h in a furnace and cooled to room temperature. The black precipitates were collected and washed with distilled water and then dried in a vacuum oven at 80 °C for 12 h. The yield of a single experiment is about 3 g.

The morphology, as shown in images a and b of Figure 1 of the as-prepared sample, was characterized by a field-emission scanning electron microscope (FE-SEM, JEOL 6340F). The low-magnification image (Figure 1a) clearly reveals that the shape of the as-prepared particles is almost hexagonal. The high-magnification image (Figure 1b) demonstrates that the hexagonally shaped particles are micrometer-scale plates with an edge length of ~200−2000 nm and the thickness of several tens of nanometers. The chemical composition of these nanoplates was further determined by energy-dispersive X-ray spectroscopy (EDS). Only peaks of the elements Sb and Te are present in the EDS spectrum with an approximate ratio of 2:3, implying the stoichiometry of Sb_2Te_3. There are no peaks from other impurities, such as Br and N, indicating that CTAB is not left on the surface of nanoplates. Powder X-ray diffraction was performed with an X-ray diffractometer (XRD, Cu Kα, Bruker AXS). Figure 1c shows the typical 2-theta XRD spectrum of the as-prepared Sb_2Te_3 nanoplates. The diffraction peaks can be indexed to the rhombohedral Sb_2Te_3 structure (JCPDS No. 71-393, $R\bar{3}m$). The peak marked with an asterisk is from excess Te.

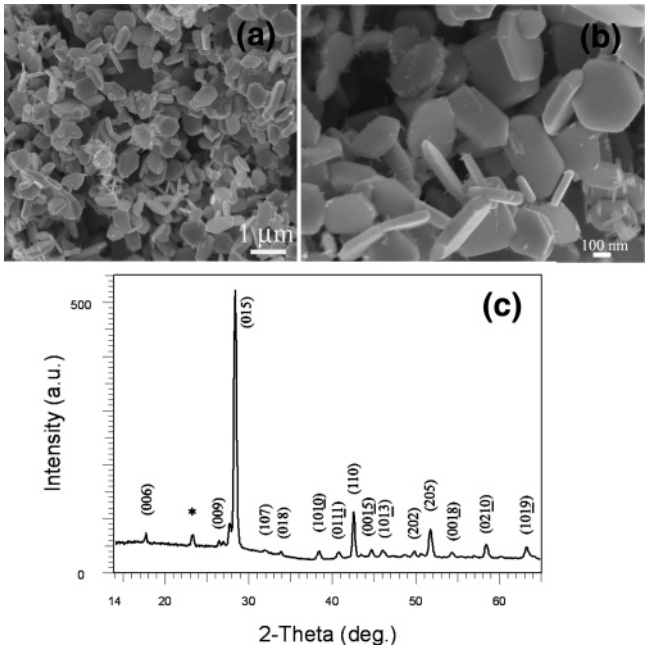

Figure 1. (a) Low- and (b) high-magnification SEM images of the as-prepared Sb_2Te_3 nanoplates. (c) XRD pattern of the as-prepared Sb_2Te_3 nanoplates.

Figure 2 shows typical TEM images of the Sb_2Te_3 nanoplates prepared by using 1.1 mmol of CTAB during experiment. Figure 2a shows the TEM image of a single hexagonal Sb_2Te_3 nanoplate with the HRTEM image (Figure 2b) of the selected area marked by the square in Figure 2a. The SAED (inset in Figure 2a) pattern was obtained by aligning the electron beam perpendicular to the face of this plate. The hexagonally symmetric spots pattern indicates the single crystallinity and can be indexed based on a rhombohedral cell with a lattice parameter of $a = 4.264$ and $c = 30.458$ Å. The clear lattice fringes shown in Figure 2b indicate that the nanoplate is highly crystallized. The spacing of 0.212 nm corresponds to the (110) planes of Sb_2Te_3. Figure 2c shows the TEM image of another Sb_2Te_3 plate. Interestingly, although the planar dimension is more than 4 μm, the plate is transparent under the electron beam, indicating that the plate is very thin. The SAED pattern shown in the Figure 2d inset also exhibits a hexagonal symmetry diffraction spot pattern. The HRTEM image (Figure 2d) of a selected area

10.1021/ja054861p CCC: $30.25

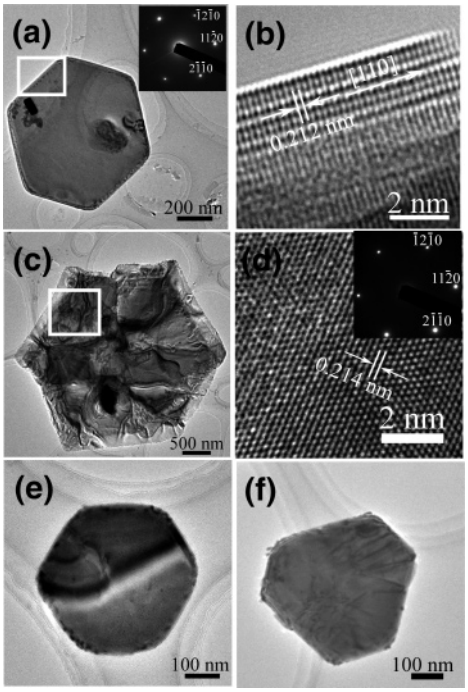

Figure 2. (a) Typical TEM image of an individual hexagonal nanoplate. (b) HRTEM image of the marked area shown in (a). Both the HRTEM image (b) and the SAED pattern (a) show that the nanoplate is a single crystal. (c) The TEM image of another Sb_2Te_3 nanoplate with the planar dimension more than 4 μm. (d) HRTEM image of the square area indicated in (c). Both the HRTEM and the SAED pattern show that the nanoplate is a highly crystallized single crystal. (e) A truncated hexagonal plate. (f) A truncated triangular Sb_2Te_3 nanoplate.

marked by a square in Figure 2c shows the clear lattice fringes with a spacing of 0.214 nm. In our TEM observations, some nanoplates have the truncated hexagonal and triangular shape, as shown in panels e and f of Figure 2, respectively. TEM observations indicated that there were a few Te particles on the surface of some Sb_2Te_3 plates, as shown in Figure 2a; this was why we observed one Te peak in the XRD (Figure 1c).

Further studies indicate that the concentration of CTAB plays an important role in the formation of hexagonally shaped Sb_2Te_3 nanocrystals. The Sb_2Te_3 nanocrystals prepared without adding CTAB are mainly composed of particles with irregular shapes. Upon adding 0.275 mmol of CTAB, the platelike Sb_2Te_3 nanocrystals with still irregular shape are formed. With CTAB concentration increased to 0.55 mmol, truncated triangular Sb_2Te_3 nanoplates are formed, but most nanoplates have irregular shape. When CTAB concentration increases to 1.1 mmol, the product is composed of mainly hexagonally shaped nanoplates.

From analysis of our above experiments, it is obvious that addition of CTAB leads to formation of Sb_2Te_3 nanoplates. Therefore, it is reasonably concluded that the cationic surfactant, CTAB, plays the critical role for the formation of single-crystal Sb_2Te_3 nanoplates. Our results seem to confirm the conclusion by Pileni et al. that the formation of faceted nanocrystals is related to selective adsorption of ions and their respective counterions on the crystal faces during the growth.[18] In our case, at the initial stage, the dominant process is the formation of tiny Sb_2Te_3 crystal nuclei. With time going on, these tiny nuclei, which are fixed by CTAB molecules, coalesce with adjacent ones, decreasing their surface energy and enhancing platelike nanocrystal production. During the crystal growth, we propose that the binding between CTAB and Sb_2Te_3 inhibits crystal growth randomly and favors platelike single-crystal growth with their preferred facets. With CTAB concentration increasing from 0.275 to 1.1 mmol, the effect of selective adsorption of CTAB molecules and their respective counterions on Sb_2Te_3 crystal faces induces higher nanocrystal surface coverage and favors a large-scale production of hexagonally shaped nanoplates. However, when the concentration of CTAB is higher than 1.1 mmol, more irregular nanoparticles appear with a large size ranging from several tens to hundreds of nanometers, accompanied with a few irregular plates, indicating that more CTAB molecules will reduce the products' size and make them irregular. On the basis of the above experimental results and analysis, we propose a possible mechanism to illustrate the formation of the hexagonally shaped Sb_2Te_3 nanoplates, which mainly comprises two processes: (i) the formation of the small Sb_2Te_3 clusters as the nascent crystal nuclei; and (ii) the subsequent crystal growth to form faceted (hexagonal) nanoplates from these nuclei. Another possible mechanism of forming such hexagonal Sb_2Te_3 nanoplates may be due to its anisotropic structure. Sb_2Te_3 possess a layer crystal structure similar to that of Bi_2Te_3. This intrinsic crystal property may dominate the shape of the primary Sb_2Te_3 particles (i.e., platelet seed), resulting in the formation of hexagonal platelike crystals, which is similar to the formation of Bi_2Te_3 hexagonal nanoplates.[16]

In summary, micrometer-sized hexagonal single-crystalline Sb_2Te_3 nanoplates can be synthesized on a large scale by a solvothermal route. The experimental results showed that the concentration of CTAB played a key role in the formation of nanoplates. The as-prepared Sb_2Te_3 nanoplates are highly crystallized single crystals. This new nanostructure may find applications in enhancing the TE performance.

Acknowledgment. This work was supported by Intel.

References

(1) Hicks, L. D.; Dresselhaus, M. S. *Phys. Rev. B* **1993**, *47*, 12727.
(2) Hicks, L. D.; Dresselhaus, M. S. *Phys. Rev. B* **1993**, *47*, 16631.
(3) Harman, T. C.; Taylor, P. J.; Spears, D. L.; Walsh, M. P. *J. Electron. Mater.* **2000**, *29*, L1−L4.
(4) Hicks, L. D.; Harman, T. C.; Sun, X.; Dresselhaus, M. S. *Phys. Rev. B* **1996**, *53*, R10493.
(5) *CRC Handbooks of Thermoelectrics*; Rowe, D. M., Ed.; CRC Press: Boca Raton, FL, 1995.
(6) Venkatasubramaniam, R.; Siivola, E.; Colpitts, T.; Quinn, B. O. *Nature* **2001**, *413*, 597.
(7) Jin, C. G.; Zhang, G. Q.; Qian, T.; Li, X. G.; Yao, Z. *J. Phys. Chem. B* **2005**, *109*, 1430.
(8) Chen, S.; Carroll, D. L. *Nano Lett.* **2002**, *2*, 1003.
(9) Yener, D. O.; Sindel, J.; Randall, C. A.; Adair, J. H. *Langmuir* **2002**, *18*, 8692.
(10) Maillard, M.; Giorgio, S.; Pileni, M.-P. *Adv. Mater.* **2002**, *14*, 1084.
(11) Hao, E.; Kelly, K. L.; Hupp, J. T.; Schatz, G. C. *J. Am. Chem. Soc.* **2002**, *124*, 15182.
(12) Simakin, A. V.; Voronov, V. V.; Shafeev, G. A.; Brayner, R.; Bozon-Verduraz, F. *Chem. Phys. Lett.* **2001**, *348*, 182.
(13) Zhou, Y.; Wang, C. Y.; Zhu.; Chen, Z. Y. *Chem. Mater.* **1999**, *11*, 2310.
(14) Ibano, D.; Yokota, Y.; Tominaga, T. *Chem. Lett.* **2003**, *32*, 574.
(15) Sun, X.; Dong, S.; Wang, E. *Angew. Chem., Int. Ed.* **2004**, *46*, 6360.
(16) Lu, W.; Ding, Y.; Chen, Y.; Wang, Z. L.; Fang, J. *J. Am. Chem. Soc.* **2005**, *127*, 10112.
(17) Wang, D.; Yu, D.; Mo, M.; Liu, X.; Qian, Y. *J. Cryst. Growth* **2003**, *253*, 445.
(18) Pileni, M. P. *Nat. Mater.* **2003**, *2*, 145.

JA054861P